Hindawi Publishing Corporation
International Journal of Manufacturing Engineering
Volume 2014, Article ID 261349, 13 pages
http://dx.doi.org/10.1155/2014/261349

Research Article

Analyzing the Effectiveness of Microlubrication Using a Vegetable Oil-Based Metal Working Fluid during End Milling AISI 1018 Steel

Vasim Shaikh,[1] Nourredine Boubekri,[2] and Thomas W. Scharf[3]

[1] *Department of Applied Engineering, Safety and Technology, Millersville University of Pennsylvania, Millersville, PA 17551, USA*
[2] *Department of Engineering Technology, University of North Texas, Denton, TX 76207, USA*
[3] *Department of Materials Science and Engineering, University of North Texas, Denton, TX 76207, USA*

Correspondence should be addressed to Nourredine Boubekri; boubekri@unt.edu

Received 8 November 2013; Revised 18 March 2014; Accepted 21 March 2014; Published 15 April 2014

Academic Editor: Gilles Dessein

Microlubrication minimizes the exposure of metal working fluids to the machining operators leading to an economical, safer, and healthier workplace environment. In this study, a vegetable oil-based lubricant was used to conduct wear analysis and to analyze the effectiveness of microlubrication during end milling AISI 1018 steel. A solid carbide cutting tool with bright oxide finish was used with varying cutting speed and feed rate having a constant depth of cut. Abrasion was the dominant wear mechanism for all the cutting tools under consideration. Other than abrasion, sliding adhesive wear of the workpiece materials was also observed. The scanning electron microscope investigation of the used cutting tools revealed microfatigue cracks, welded microchips, and unusual built-up edges on the cutting tools flank and rake side. A full factorial experiment was conducted and regression models were generated for both the sides of tool flank wear. The study shows that with a proper selection of the cutting parameters it is possible to obtain higher tool life.

1. Introduction

Metal working fluids (MWFs) are used to cool and lubricate the tool/workpiece interface during machining. The MWFs perform several important functions including reducing the friction-heat generation and dissipating generated heat at tool/workpiece interface which results in the reduction of tool wear. MWFs also flush the chips away from the tool and clean the workpiece causing less built-up edge (BUE). Therefore, MWFs cannot be completely avoided; however, their exposure to machine operators is a cause of growing occupational health hazards. U.S. National Institute for Occupational Safety and Health (NIOSH) recommends that occupational permissible exposure limits to MWF aerosols be limited to 0.4 mg/m^3 of thoracic particulate mass which corresponds to approximately 0.5 mg/m^3 of total particulate mass as a time-weighted average (TWA) concentration for up to 10 hours per day during a 40-hour workweek [1]. However, the oil mist level in the U.S. automotive parts manufacturing facilities has been estimated to be 20–90 mg/m^3 with the use of conventional lubrication by flood coolant [2]. The exposure to such amounts of metal working fluid may contribute to adverse health effects and safety issues, including toxicity, dermatitis, respiratory disorders, and cancer [3]. Also, the costs related to the use of MWFs range from 7 to 17% of the total costs of the manufactured workpiece [4] as compared to the tool cost which is only about 2–4% [5]. Microlubrication is also known as "minimum quantity lubrication" (MQL) and "near-dry machining." In microlubrication, a small amount of cutting fluid, usually 2–100 milliliters per hour mL/hr [6–8] in the form of aerosol is delivered to the cutting tool/workpiece interface and does not recirculate through the lubrication system.

It is almost all evaporated at the point of application. Hence no recirculation is required. It is important however to ensure an efficient extraction of aerosol from the machine. In a flood application, the same coolant is recirculated through the system, filtered, and used again [9]. The lubrication is

obtained via the lubricant, and the cooling is achieved by the pressurized air that reaches the cutting surface in a microlubrication application. Further, microlubrication reduces induced thermal shock and helps to increase the workpiece surface integrity in situations of high tool pressure [10]. The efficiency of a machining process depends on the tribological conditions which lower the tool wear rate obtained by the cooling and lubricating effectiveness of the cutting fluid. The main objective of this work is to investigate the effectiveness of microlubrication during end milling AISI 1018 steel with a solid carbide cutter under varying cutting speed, feed rate levels, and a constant depth of cut. A full factorial experiment and regression models for the tool flank wear are generated.

2. Experimental Methods

End milling experiments were carried out on a Mori Seiki computer numerical control (CNC) Dura vertical 5060 milling machine with a spindle power of 15 HP and a maximum spindle speed of 10,000 revolutions per minute (RPM). Figure 1 shows the machining set-up. The nozzle was positioned approximately 15 cms from the cutting tool tip at an angle of 45°. AISI 1018 steel was used as workpiece material. The alloy can be easily formed, machined, welded, and fabricated. The alloy is a free machining grade that is often employed in high volume screw machine parts applications and is commonly employed in shafts, spindles, pins, rods, sprocket assemblies, and a wide variety of component parts.

A Kuroda Ecosaver KEP3 microlubrication unit was installed on the milling machine to provide a constant aerosol flow rate of 12 mL/hr through one external nozzle as shown in Figure 2. Accu-Lube LB-2000 was used as minimum quantity lubricant manufactured by ITW Rocol North America. The lubricant was specially recommended for microlubrication of ferrous and nonferrous materials. It is manufactured using renewable raw materials and is nontoxic and biodegradable. It is not diluted in water before use.

Vegetable oils are by their chemical nature long chain fatty acid triesters of glycerol and provide most of the desirable lubricant properties such as good boundary lubrication, high viscosity index, high flash point, and low volatility. These advantages are mainly due to their polar ester structure and higher molecular weight in comparison to petroleum derived hydrocarbons [11]. Vegetable oil-based MWFs are highly attractive substitutes for petroleum oil-based MWFs because they are environmentally friendly, renewable, less toxic, and readily biodegradable. As a result, vegetable oil-based MWFs are more potential candidates for use in metal working industry as MWFs [12].

It is suggested that vegetable oil-based MWFs perform better than mineral oil-based MWFs because of their lubricity. Vegetable oil carries a slight polar charge. This charge draws the vegetable oil-based MWFs molecule to a metallic surface and is tenacious enough to resist being wiped off. Mineral oil-based MWFs have no charge and, therefore, adhere less tightly to a metal surface. Also, mineral oil-based MWFs are just a straight hydrocarbon. The vegetable oil-based MWFs have functional groups containing oxygen which makes them more attractive to the metal surface and they bond more tightly making them better MWFs [13]. It is reported that vegetable oil-based MWFs increase the tool life 30% more and give better lubricity as compared to mineral oil-based MWFs.

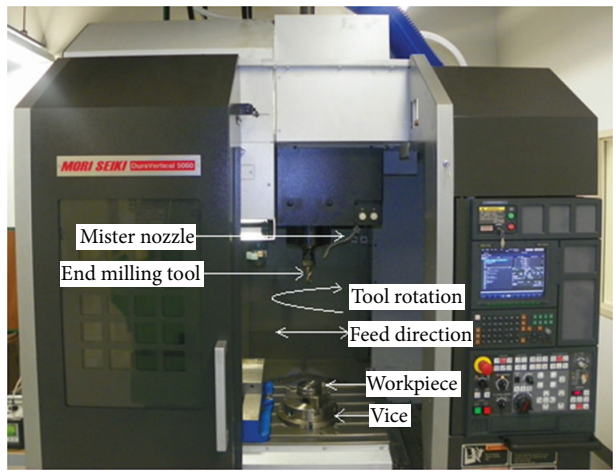

Figure 1: Machining set-up.

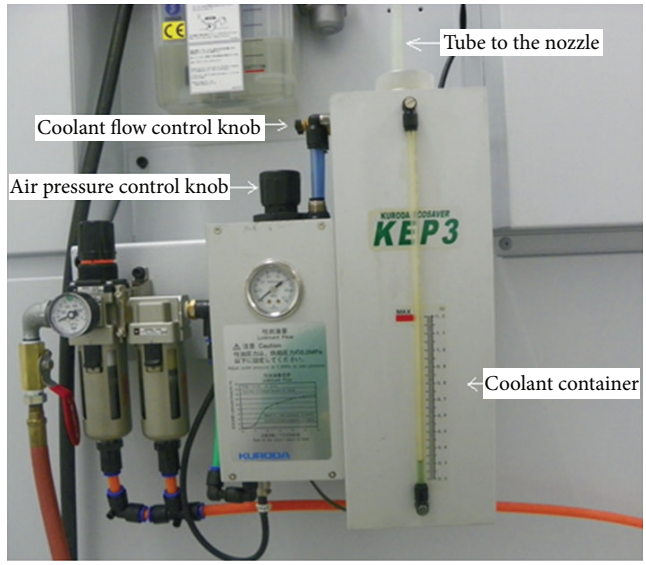

Figure 2: Microlubrication unit.

Vegetable oil-based MWFs have higher flashpoint and are more compatible with human skin than mineral oil-based MWFs. Also, vegetable oil-based MWFs are able to machine chlorine-free. Disposal costs dramatically decrease if MWFs are used without chlorine which is an inherent part of most MWFs. Vegetable oil-based MWFs also producing less mist improve the tool life and surface finish of the machined surface [14].

An exhaust pump was used to collect the mist generated during machining to replicate the exact factory production environment. End milling was carried out with cutting speeds of 24, 30, and 36 meters per minute (m/min) and feed rates of 0.15 and 0.25 millimeters per revolution (mm/rev).

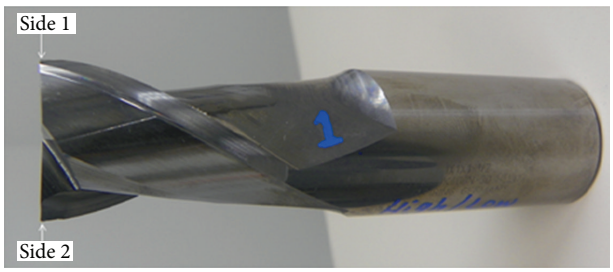

Figure 3: Cutting tool.

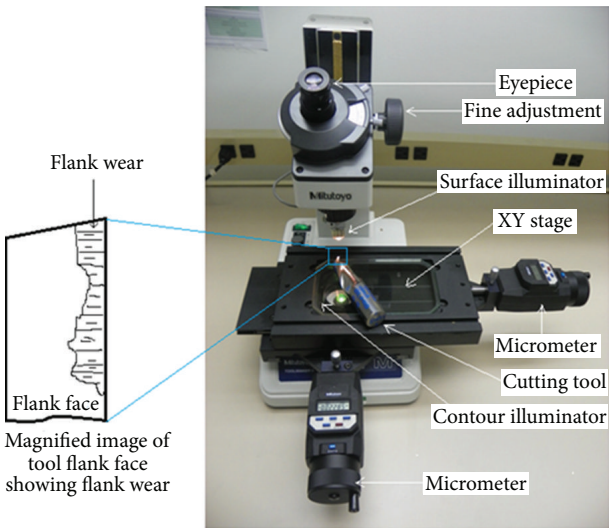

Figure 4: The Mitutoyo toolmakers microscope.

The cutting parameters were decided based on the recommendation in the ASM metal handbook for machining [15]. The axial depth of cut was 3.175 mm and the radial depth of cut was 6.35 mm. The cutting tool used in the experiment was 25.4 mm diameter of solid carbide end mill having square ends and two flutes with bright oxide finish manufactured by Guhring Inc. Figure 3 shows the cutting tool with clearly marked sides 1 and 2. The helix angle of the flute was 30° and the flute length was 38.1 mm. The radial rake angle is 9°. The radial relief is 10°.

The flank wear on both the flanks was measured at regular interval by the Mitutoyo toolmakers microscope. The microscope and a magnified inset image of the tool flank face showing the flank wear as seen from the microscope are shown in Figure 4.

The cutting tool was set on the XY stage with its flank aligned with the y-axis as seen from the eyepiece. The microscope has a contour illumination from the bottom suited for measurement and inspection of specimen contour and a surface illuminator for observation and inspection of specimen surfaces. A digital micrometer head was attached to the x- and y-axis and was set to zero. The micrometer was equipped with digital data display which gave live readings. The y-axis was carefully moved in $+y$-directions and was aligned with the maximum flank wear valley as seen on the tool from the eyepiece. Reading from the micrometer was then collected and recorded in manually.

Table 1: Factorial experiment layout of cutting speed and feed rate combination.

Solid carbide end mill	Cutting speeds (m/min)		
	24	30	36
Feed rates (mm/rev)			
0.15	24, 0.15	30, 0.15	36, 0.15
0.25	24, 0.25	30, 0.25	36, 0.25

The tool was declared failed if the flank wear of any one of the two flanks went above 0.5 mm [15]. A dual beam FEI Nova 200 NanoLab scanning electron microscope (SEM) was used to conduct the wear analysis of the cutting tool. The FEI Quanta environmental SEM (ESEM) was used to do the wear analysis of the workpiece. The secondary electron detector (ETD) was used to acquire all the SEM images. The toolmakers microscope has a maximum magnification of 40x. It is only suitable to measure the flank wear and to have an overall impression of the tool failure. However, SEM provides magnification which is way beyond the capability of the toolmakers microscope making it suitable to conduct the wear analysis of the cutting tool and the workpiece. The Vickers microhardness measurements were carried out using the Shimadzu dynamic ultramicrohardness tester model number DUH-211S. The hardness tester used a 115° standard pyramid indenter. The normal load used was 300 mN. The indentation depth is automatically measured as the indenter is pressed against the specimen eliminating human error. This allows dynamic measurement of changes that occur in the specimen's resistance to deformation during the indentation process. The hardness tester measures dynamic hardness and evaluates the hardness that corresponds to both plastic and elastic deformation. Indents were made at an increment of 10 μm up to the bulk of the material as shown in Figure 5. Adequate spacing of 50 μm was kept between two indents to avoid any possible alteration in readings due to the deformation caused by the earlier indent.

3. Design of Experiments

The study was conducted using a randomized factorial design. Full factorial design was used in the current study because the numbers of runs are uncertain as they were based on the tool failure which cannot be predetermined. Table 1 shows the factorial experiment with six cutting speed and feed rate combinations. The purpose to conduct a full factorial experiment was to effectively investigate the main effects as well as the interaction among the independent variables (i.e., cutting speed and feed rate). Each combination (i.e., treatment) was carried out only once, and there were no replicates. The experiment was fully randomized. An analysis of variance (ANOVA) was carried out for flank wear and F-ratios were calculated. All collected data were recorded using Microsoft Excel and transferred to Design Expert 8.0 analytical software for the ANOVA analyses.

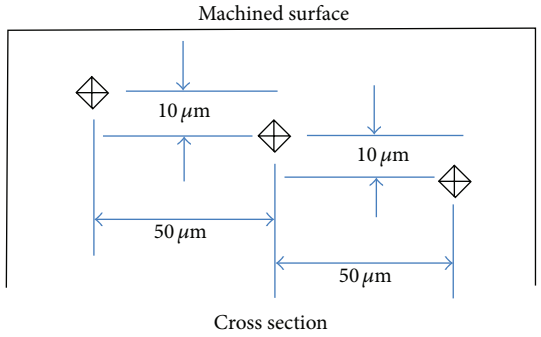

Figure 5: Schematics of the Vickers microhardness indenter.

3.1. ANOVA Assumptions

(1) Individual differences and errors of measurement are normally distributed within each group.

(2) Size of the variance, distribution of individual differences, and random errors are identical in each group.

(3) Individual differences and errors of measurement are independent from group to group.

3.2. Hypothesis

(1) *Null Hypothesis*. There is no significant difference between the responses (i.e., tool wear) obtained by varying the individual input variables levels (i.e., cutting speed and feed rate).

(2) *Alternate Hypothesis*. There is a significant difference between the responses (i.e., tool wear) obtained by varying the individual input variables levels (i.e., cutting speed and feed rate).

4. Results and Discussions

A standard technique used to check the normality assumption is to construct a normal probability plot [16]. The normal probability plot determines if the distribution of data approximates a normal distribution. In the ANOVA, the normal probability plot is usually more effective and straightforward when it is done with residuals.

The normal probability plot of residuals for both the flank wear sides is shown in Figures 6 and 7. The residual is the difference between the actual and predicted response values. The normal probability plot with a general straight line pattern indicates that the residuals follow a normal distribution. The far points which are slightly scattered do not follow any significant pattern. The analysis of variance is supposed to be robust for the normality assumption.

Figures 8 and 9 show plots of residuals versus predicted values which were used to test the assumption of constant variance for both sides 1 and 2 of the flank wear, respectively. To fulfill the test, these plots should be a random scatter. The constant variance in the data demonstrates that the data does not follow a particular pattern, indicating constant variance.

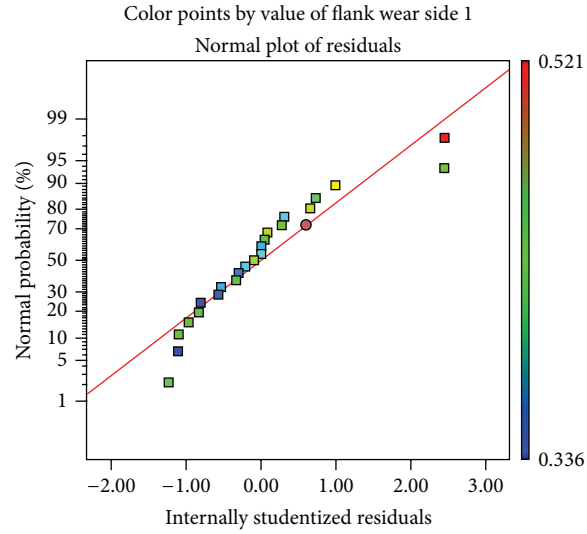

Figure 6: Normal plots of residual in data for flank wear side 1.

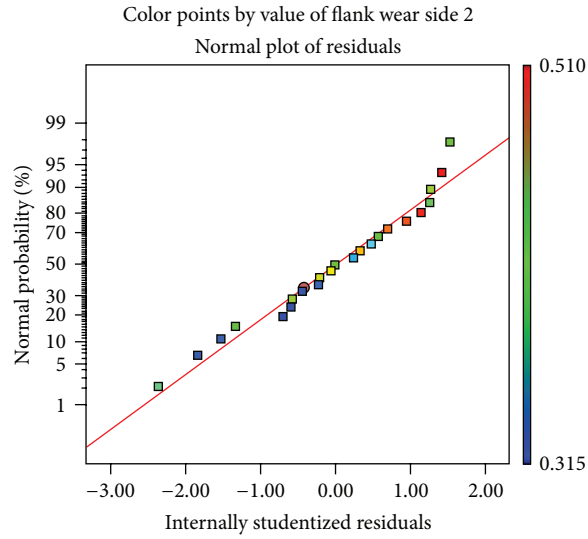

Figure 7: Normal plots of residual in data for flank wear side 2.

The ANOVA for flank wear side 1 is shown in Table 2. The model provided an F value of 10.57 which indicates that the model is statistically significant based on a 95% confidence level. The resulting R-squared value indicates that the model is able to predict 61.32 percent of the variation in the data. The remaining percent is considered noise and may not be predicted by this model, the sources of which may be manual variations while taking flank wear readings, machine vibrations, variations within the tools, and workpiece materials. The "Adeq Precision" measures the signal-to-noise ratio. The ratio of 7.85 indicates an adequate signal. Hence, the model can be used as a good predictor of the flank wear side 1 as a result of changing the cutting speed and feed rate levels. The resulting regression model is shown below.

Flank wear side 1 $= +0.5857 - (9.64E - 03 \times \text{speed}) - (0.2434 \times \text{feed}) + (0.0302 \times \text{speed} \times \text{feed})$.

Table 2: Analysis of variance for flank wear side 1.

ANOVA for selected factorial model [partial sum of squares—type III]						
Source	Sum of squares	df	Mean square	F value	P value Probability > F	
Model	0.037	3	0.012	10.57	0.0002	Significant
A speed	$6.99E-03$	1	$6.99E-03$	6.01	0.0236	
B feed	0.020	1	0.020	17.21	0.0005	
AB	$1.23E-03$	1	$1.23E-03$	1.06	0.3162	
Pure error	0.018	18	$1.02E-03$			
Cor total	0.060	23				

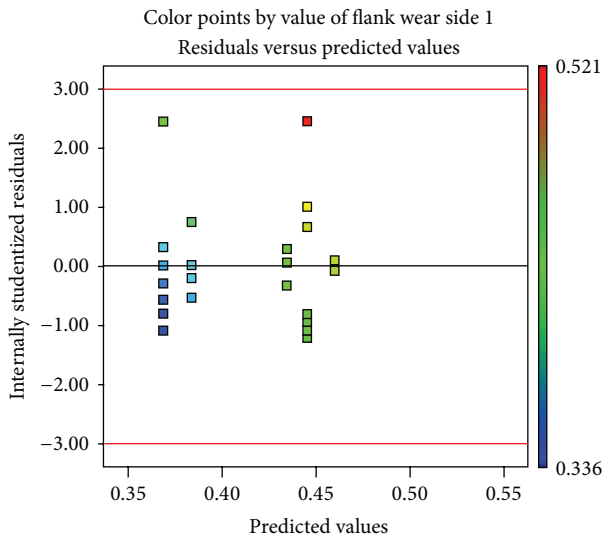

Figure 8: Constant variance in data for flank wear side 1.

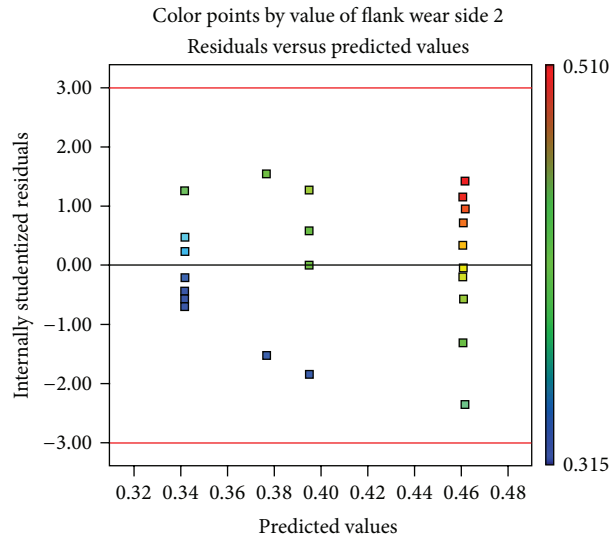

Figure 9: Constant variance in data for flank wear side 2.

Similarly, the ANOVA for flank wear side 2 is shown in Table 3. The model provided an F value of 8.27 which indicates that the model is statistically significant based on a 95% confidence level. The resulting R-squared value indicates that the model is able to predict 55.38 percent of the variation in the data. The remaining percent is considered noise and may not be predicted by this model, the sources of which may be the same as given for flank wear side 1. The "Adeq Precision" measures the signal-to-noise ratio. The ratio of 5.67 indicates an adequate signal. Hence, the model can be used as a good predictor of the flank wear side 2 as a result of changing the cutting speed and feed rate levels. The resulting regression model is shown below.

Flank wear side 2 = $+0.3447 + (7.36E-03 \times \text{speed}) + (0.3654 \times \text{feed}) - (0.0400 \times \text{speed} \times \text{feed})$.

The robustness of the regression models was validated by comparing the computed model values to the actual experimental values as shown in Table 4.

Figures 10 and 11 show the tool life in minutes and material removal volume (MRV) in mm^3 for different cutting speed and feed rate combinations, respectively. The MRV is the product of the length of cut and axial and radial depth of cut multiplied by the number of workpieces taken by the cutting tool to fail. Cutting with lower feed rate resulted in prolonged tool life and the highest MRV whereas cutting with higher feed rates decreased the tool life and MRV significantly. The cutting performance under microlubrication was approximately five times better in terms of tool life

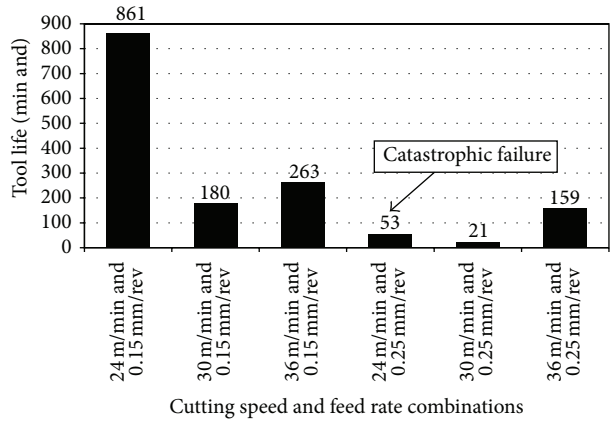

Figure 10: Tool life for different cutting speed and feed rate combinations.

Table 3: Analysis of variance for flank wear side 2.

ANOVA for selected factorial model [partial sum of squares—type III]						
Source	Sum of squares	df	Mean square	F value	P value Probability > F	
Model	0.054	3	0.018	8.27	0.0009	Significant
A speed	$2.27E-04$	1	$2.27E-04$	0.11	0.7491	
B feed	0.032	1	0.032	14.76	0.0010	
AB	$2.16E-03$	1	$2.16E-03$	1.00	0.3290	
Pure error	0.031	18	$1.72E-03$			
Cor total	0.097	23				

Table 4: Comparison of experimental and predicted flank wear values.

Flank wear side	Cutting speed and feed rate combination	Experimental mean value (mm)	Predicted value (mm)	% error
1	24 m/min and 0.15 mm/rev	0.43	0.42	+2.3
	36 m/min and 0.25 mm/rev	0.44	0.45	−2.2
2	24 m/min and 0.15 mm/rev	0.46	0.43	+6.9
	36 m/min and 0.25 mm/rev	0.34	0.34	0.0

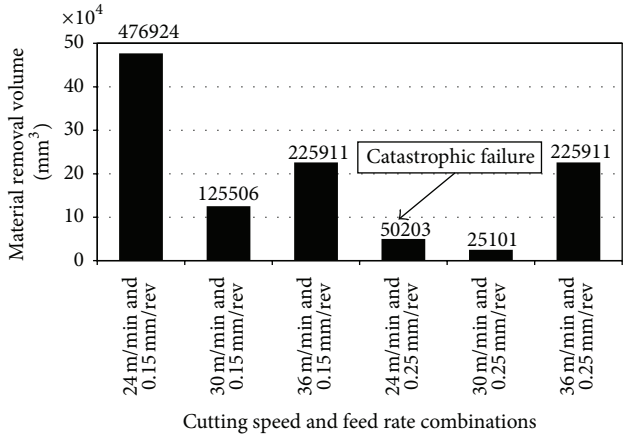

Figure 11: Material removal volume for different cutting speed and feed rate combinations.

and two times better in terms of MRV under low cutting speed and feed rate combination (i.e., 24 m/min and 0.15 mm/rev) as compared to high cutting speed and feed rate combination (i.e., 36 m/min and 0.25 mm/rev). Lower cutting speed produces lower revolutions per minute (RPM) of the spindle. Lower spindle RPM combined with lower feed rates produces more chips and higher MRV and vice versa. The highest tool life was realized using treatment at 24 m/min and 0.15 mm/rev. The tool failed after 861 minutes of machining at this treatment. Due to the lower cutting speed and feed rate [17], it is hypothesized that the aerosol particle produced by microlubrication easily penetrated through to the tool/workpiece interface [18], lubrication occurs by diffusion through the workpiece, and the cutting fluid reacts to form a boundary layer of solid-film lubricant [19]. This led to the cooling of the cutting tool and simultaneously the lubrication of the tool/workpiece interface. At low cutting speed, the cutting temperature is also expected to be low as compared to the other cutting speed and feed rate combinations [19–21]. This also contributes to the increase in tool life.

But it was observed that the MRV for cutting speed of 36 m/min was identical for both the feed rates of 0.15 and 0.25 mm/rev used in the study. This is because feed rate is more significant parameter than the cutting speed in controlling the MRV [22]. Also, high spindle speed in combination with high feed rate causes evaporative cooling and enhances the cutting tool performance resulting in higher MRV [6]. One other fact to consider is that both the cutting combinations machined exactly the same number of workpieces. However, the feed rate of 0.15 mm/rev being slower exhibited a higher tool life in minutes than at 0.25 mm/rev.

The lowest tool life was realized using treatment at 30 m/min and 0.25 mm/rev. The tool failed only after 21 minutes of machining. Several reasons are hypothesized to have contributed to the lower tool life. Due to high feed rate, the cutting fluid cannot effectively cool and lubricate the cutting zone leading to higher temperatures. The tip of the tool is highly sensitive at high temperature [23]. Also, under high feed rate, the subsurface of the workpiece is harder, as shown in Figure 12, due in part to work hardening resulting in earlier tool failure.

It was also observed that the tool life when machining at the cutting speed of 30 m/min and feed rate of 0.25 mm/rev was lower than when machining at the highest speed of 36 m/min for the same feed rate. It is hypothesized that machining at the cutting speed of 36 m/min causes evaporative cooling of the fluid droplets that impact the target surface enhancing the heat transfer from the tools cutting edge surface as compared to the cutting speed of 30 m/min. The vapor phase near the vicinity of the cutting edge is then continuously removed by the air stream carrying the MQL fluid along with the higher cutting speed of 36 m/min, allowing access for fresh cutting fluid droplets to hit the

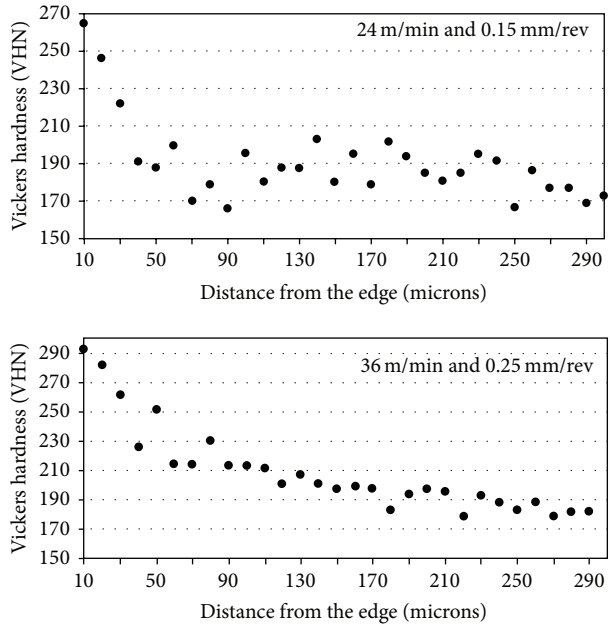

Figure 12: Microhardness depth profile of cross section for treatment at 24 m/min and 0.15 mm/rev and 36 m/min and 0.25 mm/rev.

surface required to be cooled [6]. This phenomenon of evaporative cooling is responsible for the higher tool life at the cutting speed of 36 m/min as compared to 30 m/min. This cooling effect helps the cutting tool to perform with a tool life of 159 min. But at the cutting speed of 30 m/min, this cooling effect is less dominant giving a tool life of only 21 min.

All the cutting tools under consideration failed with gradual abrasive wear except for treatment at 24 m/min and 0.25 mm/rev, which underwent a catastrophic failure. Figures 13(a)–13(f) show the cutting tool at failure for treatment at 24 m/min and 0.15 mm/rev, treatment at 36 m/min and 0.15 mm/rev, treatment at 30 m/min and 0.25 mm/rev, treatment at 36 m/min and 0.25 mm/rev, treatment at 30 m/min and 0.15 mm/rev, and treatment at 24 m/min and 0.25 mm/rev, respectively. Gradual abrasion of the cutting tool edge has been reported in other studies related to machining steels [24–26]. However, no study has been reported to date on end milling AISI 1018 steel under microlubrication.

Figure 14 shows the cutting tool for treatment at 24 m/min and 0.25 mm/rev, which exhibited catastrophic failure. The massive chipping shown in the figure is the reason for the failure of the tool. Two main conditions or causes of chipping are mechanical shock (i.e., impact by interrupted cutting as in milling) and thermal fatigue (i.e., cyclic variation in temperature of the tool in interrupted cutting) [27]. Chipping can also be caused by high temperatures at higher speed or higher feed rate conditions. Failure is linked to the fatigue crack promoted by cyclic variation of the tool temperature during machining [28].

SEM examination enabled the cutting edge of the flank and the rake side of the cutting tool to be analyzed and revealed that various other microwear mechanisms were activated at different cutting speed and feed rate levels. The cutting speed and feed rate level of 36 m/min and 0.25 mm/rev as well as 24 m/min and 0.15 mm/rev were selected for further SEM analysis. Based on SEM observation, two-body abrasion wear mode is likely dominant as shown in Figures 15(a) and 15(b). Microgrooves are formed which expose the tool substrate. This is due to the high temperature resulting from the high cutting speed and feed rate levels of 36 m/min and 0.25 mm/rev [29].

In addition, chips form a foreign body and slide between the tool rake wear and the workpiece activating sliding wear as shown in Figure 16 and causing the tool tip to gradually wear out at the contact zone. In low carbon steel, the softer ferrite phase coexist with the patches of harder pearlite phase. During machining, these pearlite patches "break off" from the workpiece and work as an abrasive particle, abrading the tool surface [30].

Figure 17 shows development of microfatigue crack near to the cutting edge resulting in the weakening of the bright oxide finish coating and decreasing the local hardness. This may finally result in the removal of the oxide finish from the tool and exposure of the tool substrate [31]. These results indicate that wear mechanism started by severe microabrasion leading to sliding wear, progressed to microfatigue at finish layer, and eventually caused the oxide finish layer to spall of the surface on the cutting tool.

Figures 18(a) and 18(b) show microchips being welded on rake and flank face, respectively. A higher magnification inset picture is also shown to clarify the view. It is likely that chips at higher speed and feed rate level get welded to the cutting tool because of inadequate time for the MWF to reach the cutting tool/workpiece interface [23].

Figures 19, 20, 21, and 22 show SEM images of cutting tool edges for the cutting speed and feed rate level of 24 m/min and 0.15 mm/rev. Sliding wear and nonuniform microabrasion similar to high speed and feed rate level were

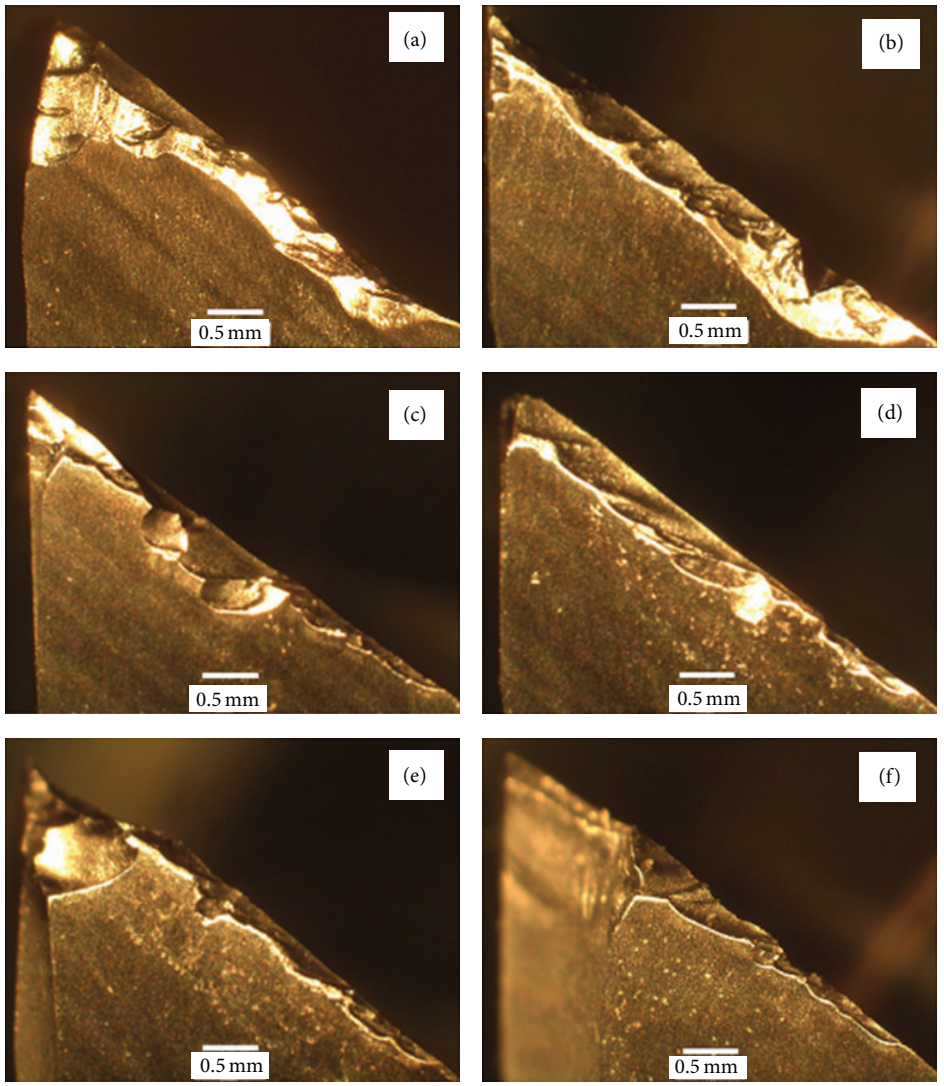

Figure 13: Optical micrograph of tool flank wear for treatment at (a) 24 m/min and 0.15 mm/rev, (b) 36 m/min and 0.15 mm/rev, (c) 30 m/min and 0.25 mm/rev, (d) 36 m/min and 0.25 mm/rev, (e) 30 m/min and 0.15 mm/rev, and (f) 24 m/min and 0.25 mm/rev.

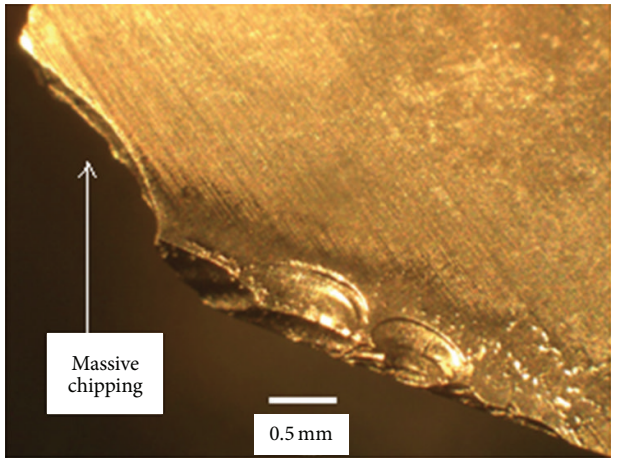

Figure 14: Optical micrograph of tool rake for treatment at 24 m/min and 0.25 mm/rev.

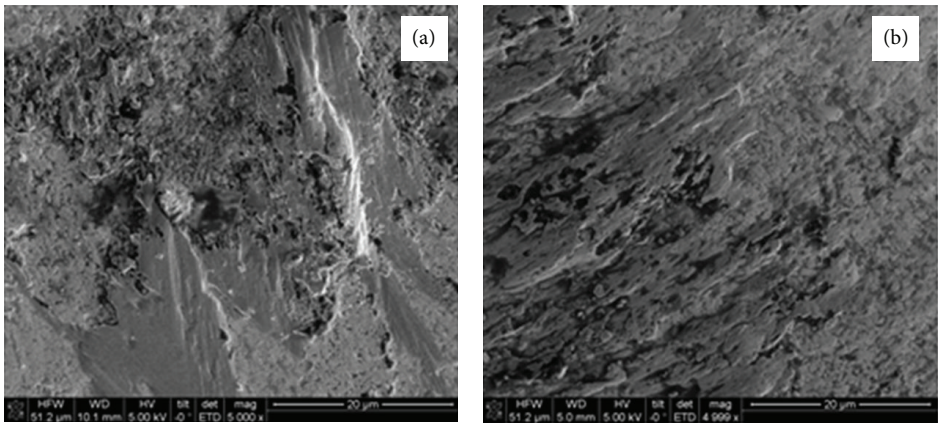

Figure 15: SEM micrograph of tool for treatment at 36 m/min and 0.25 mm/rev showing nonuniform microabrasion. (a) Rake and (b) flank.

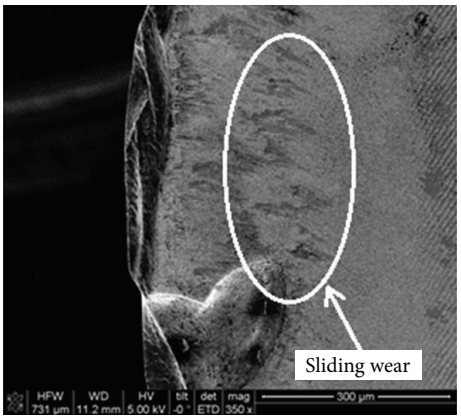

Figure 16: SEM micrograph of tool rake for treatment at 36 m/min and 0.25 mm/rev showing sliding wear.

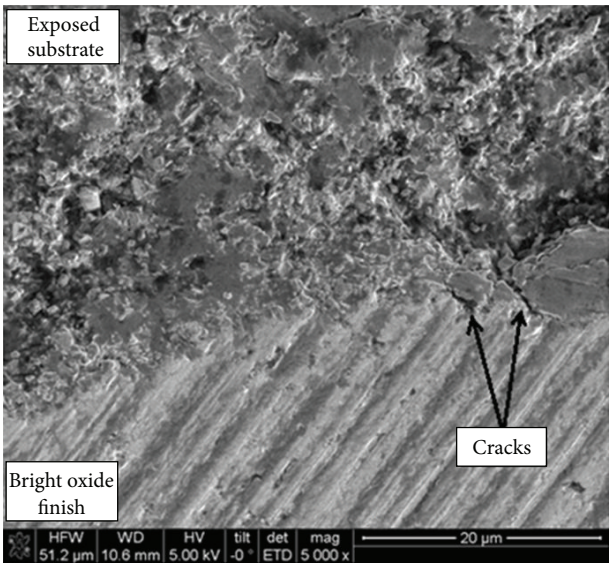

Figure 17: SEM micrograph of tool rake for treatment at 24 m/min and 0.15 mm/rev showing microfatigue crack.

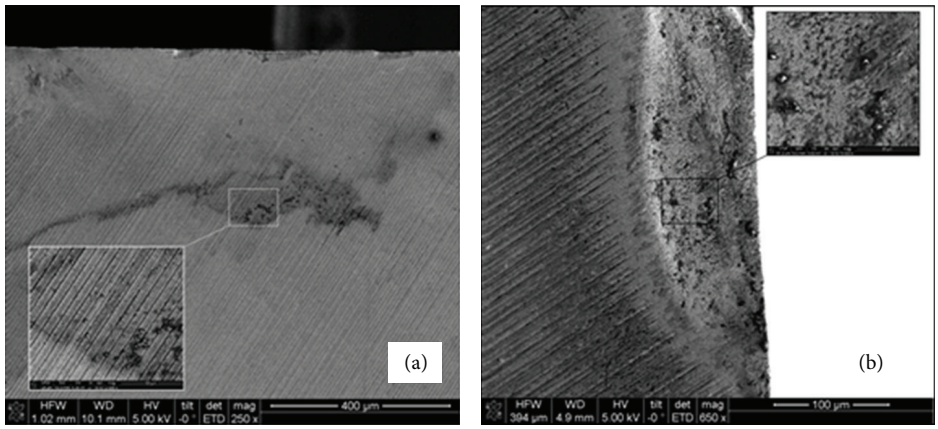

Figure 18: SEM micrograph of tool for treatment at 36 m/min and 0.25 mm/rev showing welded microchips. (a) Rake and (b) flank.

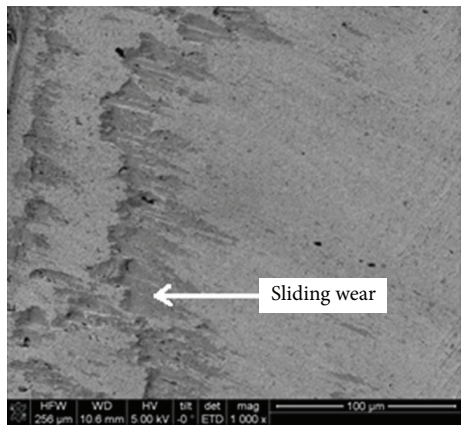

Figure 19: SEM micrograph of tool rake for treatment at 24 m/min and 0.15 mm/rev showing sliding wear.

observed for low speed and low feed rate levels (i.e., 24 m/min and 0.15 mm/rev).

Figure 19 shows the occurrence of sliding wear having grooves parallel to the metal flow direction. Figures 20(a) and 20(b) show nonuniform microabrasion for rake and the flank side, respectively. Microfatigue cracks were not observed at this treatment. The tool flank and rake faces showed unusual build-up edge (BUE) and adhesion of workpiece material to the cutting edges for treatment at 24 m/min and 0.15 mm/rev, as shown in Figures 21 and 22, respectively. The BUE shown in Figure 22 was not a stable kind of BUE.

Figure 23 shows the SEM image of the workpiece surface for treatment at 24 m/min and 0.15 mm/rev. The images clearly show abrasive wear through the mechanism of plowing. It is hypothesized that these small fragments of workpiece materials have adhered to the cutting tool faces causing adhesive wear. However, it is to be noted that plowing did not happen consistently throughout the machined workpiece surface.

5. Conclusion

The focus of this study was to investigate the effects of microlubrication during end milling American Iron and Steel Institute (AISI) 1018 steel with a 1-inch solid carbide cutter under varying cutting speed and feed rate levels and a constant depth of cut using Accu-Lube 2000 vegetable oil-based lubricant at a constant flow rate, an air pressure of 12 mL/h, and 0.1 megapascals (MPa), respectively. Machining experiments were carried out for a total of six combinations having cutting speeds of 24, 30, and 36 meters per minute (m/min) and feed rates of 0.15 and 0.25 millimeters per revolution (mm/rev). The cutting performance under microlubrication is five times better in terms of tool life and two times better in terms of MRV under low cutting speed and feed rate combination (i.e., 24 m/min and 0.15 mm/rev) as compared to high cutting speed and feed rate combination (i.e., 36 m/min and 0.25 mm/rev) for AISI 1018 steel using a vegetable oil-based cutting fluid. Therefore, the best combination of cutting parameters that led to lower tool life was the cutting speed of 24 m/min and feed rate of 0.15 mm/rev. Massive chipping was observed at the cutting tool edge for treatment at 24 m/min and 0.25 mm/rev causing catastrophic tool failure. Gradual two-body abrasion was the dominant wear mechanism except for treatment at 24 m/min and 0.25 mm/rev where the tool underwent catastrophic failure due to massive chipping. Similar results on gradual abrasive

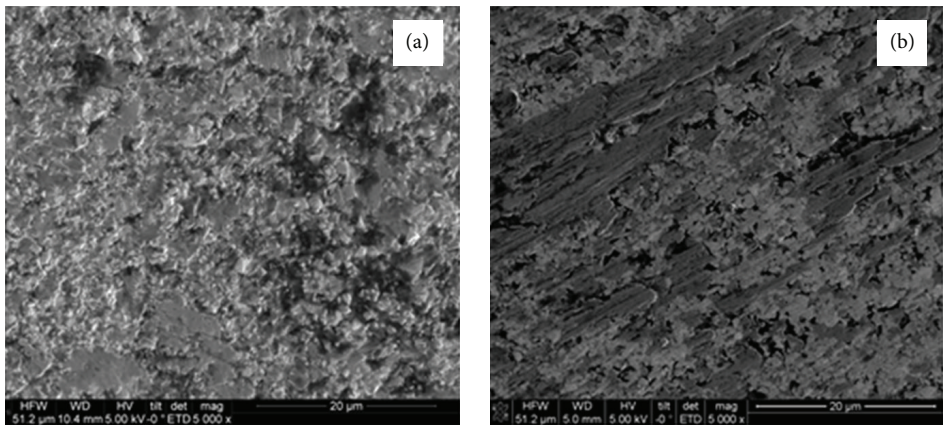

Figure 20: SEM micrograph of tool for treatment at 24 m/min and 0.15 mm/rev showing nonuniform microabrasion. (a) Rake and (b) flank.

Figure 21: SEM micrograph of tool flank for treatment at 24 m/min and 0.15 mm/rev showing adhesion.

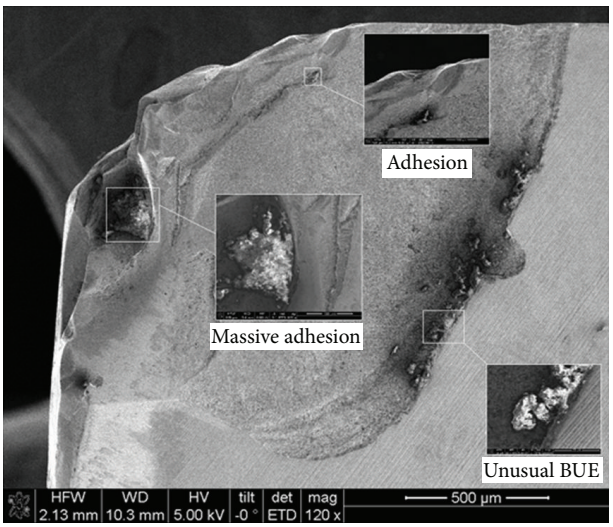

Figure 22: SEM micrograph of tool rake for treatment at 24 m/min and 0.15 mm/rev showing adhesion and built-up edge (BUE).

wear mechanism were reported in the literature [24–26] on other steels than the one investigated in this study. Exact comparison with similar grade steel cannot be done because no studies have been reported in the literature to date on end milling AISI 1018 steel under microlubrication. Other than abrasion, sliding adhesive wear of the workpiece materials was also observed. The SEM investigation of the used cutting tools revealed microfatigue cracks, welded microchips, and

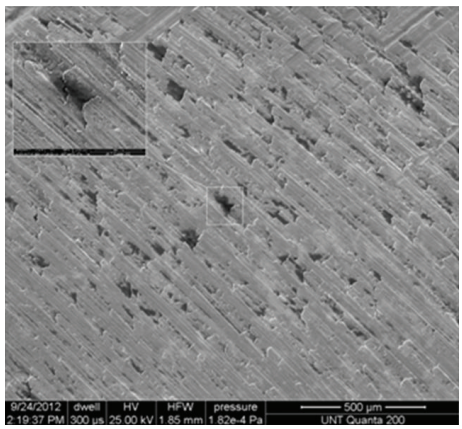

Figure 23: SEM micrograph of workpiece for treatment at 24 m/min and 0.15 mm/rev showing abrasive wear through plowing mechanism.

unusual built-up edges on the cutting tools flank and rake side. The ANOVA clearly indicated that both the cutting speed and feed rate are statistically significant factors based on a 95% confidence level for both the flank wear sides. It can be concluded that the flank wear can be predicted using the obtained regression models, under the conditions investigated in this study.

Conflict of Interests

The authors declare that there is no conflict of interests regarding the publication of this paper.

References

[1] U.S. Department of Health and Human Services, *Occupational Exposure to Metal Working Fluid*, 98-102, NIOSH Publication, 1998.

[2] E. O. Bennett and D. L. Bennett, "Occupational airway diseases in the metalworking industry. Part 1: respiratory infections, pneumonia, chronic bronchitis and emphysema," *Tribology International*, vol. 18, no. 3, pp. 169–176, 1985.

[3] N. Boubekri and V. Shaikh, "Machining using minimum quantity lubrication: a technology for sustainability," *International Journal of Applied Science and Technology*, vol. 2, pp. 111–115, 2012.

[4] K. Weinert, I. Inasaki, J. W. Sutherland, and T. Wakabayashi, "Dry machining and minimum quantity lubrication," *CIRP Annals—Manufacturing Technology*, vol. 53, no. 2, pp. 511–537, 2004.

[5] S. Zhang, J. F. Li, and Y. W. Wang, "Tool life and cutting forces in end milling Inconel 718 under dry and minimum quantity cooling lubrication cutting conditions," *Journal of Cleaner Production*, vol. 32, pp. 81–87, 2012.

[6] A. D. Jayal and A. K. Balaji, "Effects of cutting fluid application on tool wear in machining: interactions with tool-coatings and tool surface features," *Wear*, vol. 267, no. 9-10, pp. 1723–1730, 2009.

[7] S. Kurgin, G. Barber, and Q. Zou, "Cutting insert and work piece materials for minimum quantity lubrication," in *International Seminar on Modern Cutting and Measurement Engineering*, vol. 7997 of *Proceedings of the SPIE*, pp. 1–10, Beijing, China, December 2010.

[8] M. H. Sadeghi, M. J. Hadad, T. Tawakoli, A. Vesali, and M. Emami, "An investigation on surface grinding of AISI 4140 hardened steel using minimum quantity lubrication-MQL technique," *International Journal of Material Forming*, vol. 3, no. 4, pp. 241–251, 2010.

[9] V. Shaikh and N. Boubekri, "Effects of minimum quantity lubrication in drilling 1018 steel," *Journal of Manufacturing Technology Research*, vol. 1, pp. 1–14, 2010.

[10] A. Attanasio, M. Gelfi, C. Giardini, and C. Remino, "Minimal quantity lubrication in turning: effect on tool wear," *Wear*, vol. 260, no. 3, pp. 333–338, 2006.

[11] A. K. Singh and A. K. Gupta, "Metalworking fluids from vegetable oils," *Journal of Synthetic Lubrication*, vol. 23, no. 4, pp. 167–176, 2006.

[12] S. A. Lawal, I. A. Choudhury, and Y. Nukman, "Application of vegetable oil-based metalworking fluids in machining ferrous metals—a review," *International Journal of Machine Tools and Manufacture*, vol. 52, no. 1, pp. 1–12, 2012.

[13] S. Woods, "Going green," *Cutting Tool Engineering*, vol. 57, no. 2, pp. 11–13, 2005.

[14] W. R. Stott, "Environmentally friendly cutting fluids," *Gear Technology*, vol. 22, no. 2, pp. 16–18, 2005.

[15] J. R. Davis, *ASM Metals Handbook, Machining*, vol. 16, 19th edition, 1989.

[16] D. C. Montgomery, *Design and Analysis of Experiments*, John Wiley & Sons, New York, NY, USA, 5th edition, 2001.

[17] T. H. C. Childs, K. Maekawa, T. Obikawa, and Y. Yamane, *Metal Machining, Theory and Applications*, Oxford, UK, 2000.

[18] S. Min, I. Inasaki, S. Fujimura, T. Wakabayashi, and S. Suda, "Investigation of adsorption behaviour of lubricants in near-dry machining," *Proceedings of the Institution of Mechanical Engineers B: Journal of Engineering Manufacture*, vol. 219, no. 9, pp. 665–671, 2005.

[19] D. P. Adler, W. W.-S. Hii, D. J. Michalek, and J. W. Sutherland, "Examining the role of cutting fluids in machining and efforts to address associated environmental/health concerns," *Machining Science and Technology*, vol. 10, no. 1, pp. 23–58, 2006.

[20] S. M. Ali, N. R. Dhar, and S. K. Dey, "Effect of minimum quantity lubrication (MQL) on cutting performance in turning medium carbon steel by uncoated carbide insert at different speed-feed combinations," *Advances in Production Engineering & Management*, vol. 6, pp. 185–198, 2011.

[21] M. Shaw, J. Pigott, and L. Richardson, "The effect of cutting fluid upon chip-tool interface temperature," *Transaction of ASME*, vol. 73, pp. 45–56, 1951.

[22] H. Yanda, J. A. Ghani, M. N. A. M. Rodzi, K. Othman, and C. H. C. Haron, "Optimization of material removal rate, surface roughness and tool life on conventional dry turning of FCD700," *International Journal of Mechanical and Materials Engineering*, vol. 5, no. 2, pp. 182–190, 2010.

[23] N. R. Dhar, M. T. Ahmed, and S. Islam, "An experimental investigation on effect of minimum quantity lubrication in machining AISI 1040 steel," *International Journal of Machine Tools and Manufacture*, vol. 47, no. 5, pp. 748–753, 2007.

[24] H. Caliskan, C. Kurbanoglu, P. Panjan, M. Cekad, and D. Kramar, "Wear behavior and cutting performance of nanostructured hard coatings on cemented carbide cutting tools in hard milling," *Tribology International*, vol. 62, pp. 215–222, 2013.

[25] R. Suresh, S. Basavarajappa, V. N. Gaitonde, and G. L. Samuel, "Machinability investigations on hardened AISI 4340 steel using coated carbide insert," *International Journal of Refractory Metals and Hard Materials*, vol. 38, pp. 124–133, 2013.

[26] A. K. Sahoo and B. Sahoo, "Experimental investigations on machinability aspects in finish hard turning of AISI, 4340 steel using uncoated and multilayer coated carbide inserts," *Measurement*, vol. 45, pp. 2153–2165, 2012.

[27] S. Kalpakjian, *Manufacturing Engineering and Technology*, Addison-Wesley Publishing Company, New York, NY, USA, 3rd edition, 1995.

[28] R. B. Da Silva, J. M. Vieira, R. N. Cardoso et al., "Tool wear analysis in milling of medium carbon steel with coated cemented carbide inserts using different machining lubrication/cooling systems," *Wear*, vol. 271, no. 9-10, pp. 2459–2465, 2011.

[29] S. Dhiman, R. Sehgal, S. K. Sharma, and V. S. Sharma, "Machining behavior of AlSI 1018 steel during turning," *Journal of Scientific and Industrial Research*, vol. 67, no. 5, pp. 355–360, 2008.

[30] P. Kwon, "Predictive models for flank wear on coated inserts," *Journal of Tribology*, vol. 122, no. 1, pp. 340–347, 2000.

[31] K. Abu-Shgair, M. Al-Hasan, A. K. Abdul Jawwad, A. Al-Bashir, H. H. Abu-Safe, and M. H. Gordon, "Characterizing (Ti, AI)N film coating produced by inverted cylindrical magnetron sputtering for metal machining applications," *Reviews on Advanced Materials Science*, vol. 24, no. 1-2, pp. 48–55, 2010.